Submitted to 40th AIAA Thermophysics Conference, 30th October, 2007

AN INVERSE METHOD FOR NON LINEAR ABLATIVE THERMICS

INDUSTRIAL APPPLICATIONS

Stéphane Alestra*
EADS Innovation Works, Toulouse, France

Jean Collinet†
EADS Astrium Space Transportation, Les Mureaux, France

and

François Dubois‡
Conservatoire National des Arts et Métiers, Paris, France

Abstract

Thermal Protection System is a key element for atmospheric re-entry missions of aerospace vehicles. Consequently, the identification of heat fluxes is of great industrial interest and is usually based on temperature measurements. This contribution is concerned with inverse analyses of highly evolutive heat fluxes. An inverse problem is used to estimate transient surface heat fluxes (or convection coefficient), for thermally degradable material (with ablation and pyrolysis phenomena), by using time domain temperature measurements on thermal protection. The inverse problem is formulated as a minimization problem involving an objective functional, through an optimization loop. An optimal control formulation (Lagrangian, adjoint and gradient steepest descent method combined with quasi-Newton method computations) is then developed and applied. Accurate results of identification on high fluxes test cases, and good agreement for temperatures restitutions, are obtained using synthetic, noisy, on-ground and in-flight data measurements, without and with ablation and pyrolysis. First encouraging results with an automatic differentiation procedure are also presented in this paper.

* Dr Engineer, Simulation Information Technology Systems Engineering Department, EADS-IW, Toulouse, France, stephane.alestra@eads.net.

† R & D Engineer, Re-entry Systems & Technologies Department, Astrium-ST, Les Mureaux, France, jean.collinet@astrium.eads.net.

‡ Professor of Applied Mathematics, CNAM, Paris, France, fdubois@cnam.fr.

Nomenclature

A	=	Frequency factor in pyrolysis (s^{-1})
B	=	Activation temperature in pyrolysis (K)
C_p	=	Heat capacity (J/kg/K)
df	=	First derivative of *f* function
$d^2 f$	=	Second derivative of *f* function
d_r	=	Descent direction in optimization iteration r
e	=	Thickness of the one-dimensional slab
F	=	Operator of direct evolution problem
F_v	=	Pyrolysis gas formation heat (J/kg)
f	=	Discrete operator of evolution problem
H_c	=	Pyrolysis gas combustion heat (J/kg)
H_r	=	Hessian approximation at optimization *r* iteration
H_v	=	Ablation heat (J/kg)
h_g	=	Pyrolysis gas enthalpy (J/kg)
h_r	=	Athermanous enthalpy (J/kg)
h_w	=	Surface enthalpy (J/kg)
$Inst^{n+1}$	=	Solver Program instruction at time (n+1)
J (p)	=	Cost function
L	=	Lagrangian multiplyer
n	=	Time iteration
$\dot{m}_c$	=	Ablation mass flow rate ($kg/m^2/s$)
$\dot{m}_g$	=	Pyrolysis gas mass flow rate ($kg/m^2/s$)
K	=	Number of 1D Grid points

k	=	Space index
N	=	Number of time iterations
N_{op}	=	Number of optimizer iterations
n	=	Time index
PA	=	Mechanical erosion coefficient
PB	=	Normal constraint coefficient
p	=	Parameter
p^n	=	Parameter value at time n
p_{opt}	=	Optimal parameter
q_r	=	Parameter at optimizer iteration r
r	=	Optimizer iteration indice
s	=	Ablation variable
s^n	=	Ablation variable computed at time n
$\dot{s}_{meca}$	=	Mechanical Recession rate (m/s)
$\dot{s}_{chem}$	=	Chemical Recession rate (m/s)
$\dot{s}_{hy}$	=	Hydroerosion Recession rate (m/s)
T	=	Temperature
T_{opt}	=	Optimal Temperature (at optimal p)
T_0	=	Reference initial temperature (K)
T_k^n	=	Temperature computed at time n, point m
T_E	=	Mechanical erosion fictitious temperature
T_r	=	Equivalent temperature (K)
T_w	=	Surface temperature (K)
t	=	time
t_f	=	Final time
W	=	Continuous Direct state variable: temperature & ablation
w	=	Discrete Direct state variable: temperature & ablation
w^n	=	Direct state variable at time iteration n
x	=	Sensor position
x_0	=	Sensor position
z	=	Hessian intermediate function
α_0	=	Unblocked convective heat transfer coefficient (kg-s/m2)
β_n	=	Gear coefficient at time iteration n
Δt	=	Time step
ε	=	Total Emissivity
η_1	=	Pyrolysis gas blocking factor
η_2	=	Ablation gas blocking factor
θ	=	Measured temperature
θ_m^n	=	Measured temperature at time n, point m
λ	=	Thermal conductivity (W/m/K)
μ	=	Descent coefficient for optimizer
μ_r	=	Descent coefficient at optimizer iteration r
ξ	=	Reduced scaled abscissa
ρ	=	Specific Mass (kg/m^3)
ρ_c	=	Charred material densities (kg/m^3)
ρ_v	=	Virgin material densities (kg/m^3)
σ	=	Stefan-Boltzmann constant
τ	=	Mechanical erosion fictitious constraint
φ	=	Discrete Adjoint state variable: temperature & ablation
$\varphi^{n+1/2}$	=	Adjoint state variableat time n+1/2

I. Introduction

The success of atmospheric re-entry missions is bound to the design of the Thermal Protection System (TPS) of the aerospace vehicles involved. The high level of heat fluxes encountered in such missions has a direct effect on mass balance of the heat shield. Consequently, the identification of heat fluxes is of great industrial interest but is in flight only available by indirect methods based on temperature measurements. For a more detailed description of the problem, we refer to some publications on the Atmospheric Reentry Demonstrator (ARD) suborbital reentry test flown[1-3]. The difficulty with flight data is that the uncertainty on the heat flux is coupled with an uncertainty coming also from the material (thermal properties for instance). In this contribution, we restrict ourselves to a supposed well known complex degradable material (with ablation and pyrolysis) and study in details the modeling and identification of thermal fluxes.

A lot of studies on degradable materials can be found[4] for pyrolysis and ablation processes[5,6] and the corresponding applications, like on-ground validations with arc plasma torch[7], or various work on Thermal Protection Systems and reentry vehicles design[8-12].

Many authors have already adressed the so-called Inverse Heat Conduction problem, and the estimation of fluxes from temperature measurements[13-17]. Recently, 3D inverse thermal methods for non-ablative and non-pyrolysable materials have been successfully applied[18].

The inverse problem in this paper is concerned with the estimation of time domain surface heat fluxes (or convection coefficient $\alpha_0(t)$), for thermally degradable material (ablation and pyrolysis processes), on a one-dimensional slab of thickness e, by using time domain temperature measurements $\theta(t)$ on thermal protection, taken below the boundary surface, at thermocouple

position x_0, during the time interval $0 \le t \le t_f$, where t_f denotes the final time.

This inverse problem is formulated as a minimization problem involving a least square problem through an optimization loop. An optimal control formulation (Lagrangian, adjoint and gradient computations) is then applied and developed[19] for the optimal control theory[20,21] on some industrial applications of inverse problems at EADS (European Aeronautics Defense and Space Company).

We use the Monopyro direct and inverse code[22,23], which was developed at EADS Astrium-ST Les Mureaux. It is a transient one-dimensional thermal tool with one moving boundary (ablative surface) and has been used to model complex chemical processes of simultaneous heating, pyrolysis, ablation, thermal degradation behaviour of ablative materials.

The paper is structured as follows: in section II, we describe our physical model associated to the so called direct problem. In section III, we explain our inverse methodology for estimation and identification of the heat flux, using optimal control method, and analysis of optimization tools. In section IV, we emphasize on the possible use of automatic differentiation tools[24] to generate the inverse code, for this highly non linear problem. In section V, we present some numerical results on test cases with carbon/resin material for synthetic and noisy temperatures measurements and assimilation of high fluxes without and with ablation and pyrolysis. Some comparisons with experimental on-ground (JP test case) and in-flight (ARD) aerothermal measurements data, with some uncertainties on the material, are also presented.

II. Direct problem

Continuous equations

A transient one-dimensional thermal problem with one moving boundary (ablative surface) has been developed and used at EADS Astrium-ST[25,26] to model complex chemical processes of simultaneous heating, pyrolysis, ablation and thermal degradation behaviour of ablative materials. We briefly present the direct model used.

Internal energy balance (for pyrolysable ablative material) :

The internal energy balance is a transient thermal conduction equation with additional pyrolysis terms

$$\rho C_p \frac{\partial T}{\partial t} = \frac{\partial}{\partial x}\left(\lambda \frac{\partial T}{\partial x}\right) + \left[F_V + h_g - \int_{T0}^{T} A_1 dT\right]\frac{\partial \rho}{\partial t} + \frac{\partial\left(\dot{m}_g h_g\right)}{\partial x} \quad (1)$$

with x the abscissa, t the time, T (x,t) the temperature, ρ (x,t) the specific mass, C_p the heat capacity, λ the thermal conductivity, $\dot{m}_g$ the pyrolysis gas mass flow rate, h_g the pyrolysis gas enthalpy, A_1 a constant, F_v the pyrolysis gas formation heat. The rate of storage of sensible energy is balanced by the net rate of thermal conductive heat flux, the pyrolysis energy-consumption rate and the net rate of energy convected by pyrolysis gas.

Pyrolysis with internal decomposition modelled via a first-order rate process based on the Arrhenius equation

The evolution of specific mass is given by (2):

$$\frac{1}{\rho_v}\cdot\frac{\partial \rho}{\partial t} = -\left(\frac{\rho - \rho_c}{\rho_v}\right)^{np}\cdot A \cdot e^{-\frac{B}{T}} \quad (2)$$

ρ_c and ρ_v are the charred and virgin material densities, A the frequency factor in pyrolysis, B the fictitious temperature in pyrolysis, np the order of the reaction. More complex pyrolysis models can be used, for instance as proposed in literature[4].

Internal decomposition converts some of the solid into pyrolysis gas. The pyrolysis gas mass flux is related to the decomposition by the simple mass balance:

$$\frac{\partial \rho}{\partial t} = \frac{\partial \dot{m}_g}{\partial x} \quad (3)$$

The surface recession : we denote by *s* the abscissa of the moving interface (ablation value), then $\dot{s}$ is the recession rate. This physical process can be splitted in three kinds of ablation:

$$\dot{s} = \dot{s}_{meca} + \dot{s}_{chem} + \dot{s}_{hy} \quad (4)$$

The mechanical recession rate is modeled by

$$\dot{s}_{meca} = PA\left(\tau + P_e\ PB\right) e^{-\frac{T_e}{T_p}} \quad (5)$$

with T_E the mechanical erosion fictitious temperature, τ the mechanical erosion fictitious constraint, $\dot{m}_c$ the pyrolysis gas mass flow rate, PA the mechanical erosion coefficient, PB the normal constraint coefficient. The chemical recession rate $\dot{s}_{chim} = \dot{m}_c / \rho$ is most of the time a tabulated value function of

$\dot{m}_g / \alpha_0$, of temperature T and of pressure P on the material with α_0(t) the convection coefficient, or unblocked convective heat transfer coefficient (unknown for inverse problem), and $\dot{m}_c$ the ablation mass flow rate. The hydroerosion recession rate $\dot{s}_{hy}$ variable is also most of the time a tabulated value.

Surface energy balance on the moving boundary:

The conditions at the hot surface are determined by convective heating and by thermochemical interactions of the surface with the boundary-layer gas. The surface energy balance takes the following form:

$$\begin{aligned}&\alpha_0(h_r - h_w) - \varepsilon\sigma(T_w^4 - T_r^4) + \dot{m}_g\left[H_c - \eta_1(h_r - h_w)\right] \\ &+ \dot{m}_c\left[H_v - \eta_2(h_r - h_w)\right] = \lambda\frac{\partial T}{\partial x}\end{aligned} \quad (6)$$

with η_1 the pyrolysis gas blocking factor, H_c the pyrolysis gas heat combustion, $\dot{m}_c$ the ablation mass flow rate, h_r the athermanous enthalpy, h_w the surface enthalpy, η_2 the ablation gas blocking factor, H_v the ablation heat, ε the total emissivity, σ the Stefan-Boltzmann constant, T_w the surface temperature, T_r the equivalent temperature. The first term of equation (6) represents the convective heat flux. The second term represents the heat loss by re-radiation of the surface. The third and fourth terms represent the contribution of pyrolysis and ablation gas respectively. The term on the right hand of (6) represents the rate of conduction into the TPS.

We introduce $W = \begin{pmatrix} T \\ s \end{pmatrix}$ the vector of temperature and ablation, functions of time *t* and position *x*. Therefore, the direct problem can be represented in condensed vector form by the following system of coupled nonlinear time domain evolution differential equations:

$$\begin{aligned}&\frac{dW}{dt} = F(W) \\ &T(x,0) = T_0 \qquad s(x,0) = 0 \\ &t \in [0, t_f],\ x \in [s(t), e]\end{aligned} \quad (7)$$

where $F(W)$ is a non linear operator and T_0 the reference initial temperature. The other physical quantities and variables described above are hidden in the formulation of F, and in the linear system coefficients than will result from (7) after spatial and temporal discretization.

Discrete scheme

Space partial derivatives are computed with a centered finite difference type scheme[27]. The abscissa x belongs to the interval $[s(t), e]$. It is parameterized by a reduced scaled space variable $\xi \in [0,1]$:

$$x = (1-\xi)s(t) + \xi e \quad (8)$$

Then the system (7) is rewritten relatively to the variables (t, ξ) . The variable ξ is discretized with the help of K grid points. This complete set of equations has been solved numerically, for non constant time steps, using a one-dimensional two time steps Gear Scheme, which is second order accurate implicit integration scheme, with the approximation of the time derivative on two contiguous time steps $\Delta t^{n-1/2}$ and $\Delta t^{n+1/2}$, with the β_n Gear coefficient[28]:

$$\begin{aligned}&\left(\frac{dw}{dt}\right)^{n+1} \cong \beta_n \frac{w^{n+1} - w^n}{\Delta t^{n+1/2}} + (1-\beta_n)\frac{w^n - w^{n-1}}{\Delta t^{n-1/2}} \\ &\beta_n = \frac{2\Delta t^{n+1/2} + \Delta t^{n-1/2}}{\Delta t^{n+1/2} + \Delta t^{n-1/2}} \qquad 0 \le n \le N\end{aligned} \quad (9)$$

For simplicity, we explain our method on the implicit Euler scheme with a constant time step Δt . We define K the number of one-dimensional grid points, N the number of time iterations, k the space index, n the time index in the numerical scheme, $w = (w^1, ..., w^N)$ the discrete direct state variables matrix of dimension (K+1)*N, with the discrete vector $w^n = (T_1^n, T_2^n, \cdots, T_K^n, s^n)$ of dimension (K+1), T_m^n the discrete computed temperature at time n, at grid point m, for the K different points on the grid, s^n the discrete computed ablation, at time n. The equation (7) is written at time *(n+1) :*

$$\begin{aligned}&\frac{w^{n+1} - w^n}{\Delta t} = f(w^{n+1}) \\ &w^0 = 0 \qquad 0 \le n \le N\end{aligned} \quad (10)$$

We make a linearization of the equation (10) at time *n* and after some calculations, we finally obtain a forward time discrete linearized Euler scheme, with initial condition vanishing:

$$\begin{aligned}&\frac{w^{n+1} - w^n}{\Delta t} = f(w^n) + (df)(w^n)(w^{n+1} - w^n) \\ &w^0 = 0 \qquad 0 \le n \le N\end{aligned} \quad (11)$$

Note that $f(w^n)$ is a vector (K+1)*1, $(df)(w^n)$ is the linearized square matrix (K+1)*(K+1). To solve the discrete matrix problem, we use an adapted sparse solver[29]. In order to focus on the inverse procedure, we won't develop more in details the expressions of the discrete schemes, as the direct scheme is very complex, due to non linearities (complex chemical physical processes, ablation, pyrolysis), tabulated variables for the physical ablation process, and complex linearizations and discretizations**.**

III. Inverse problem

Inverse problems are concerned with the identification of unknowns and the improvement of the understanding of physical processes quantities which appear in the mathematical formulation of physical problems, by using measurements of the system response.

The inverse problem in this paper is used to estimate time domain surface heat fluxes (convection coefficient), for degradable material (ablation and pyrolysis), on a one-dimensional slab of thickness e, by using time domain temperature measurements $\theta(t)$ on thermal protection, taken below the boundary surface, at thermocouple position x_0, during the time interval $0 \le t \le t_f$, where t_f denotes the final time. The inverse problem is reformulated as a minimization problem involving a cost objective functional, through an optimization loop, requiring the computation of derivatives or gradients quantities and adjoint variables (optimal control formulation).

Discrete problem and cost function

To obtain an accurate numerical approximation of the gradient, the key strategy is to compute the exact gradient of the discretized problem, instead of applying a discretization scheme to the above systems of PDE-s[30].

Therefore the best way is to proceed to the derivation of the direct schemes. Let us consider that the time domain content of the unknown heat flux convection coefficient is represented by a vector $p = (p^1, ..., p^N)$ which is sampled over time, where the subscripts refer to the sampled time. N is the number of unknowns and time iterations. These sampled values will be the *control parameter variables* for the optimization process.

Let us define a discrete scalar inner product of two discrete vectors $a^n = (a_1^n, \cdots, a_K^n)$ and $b^n = (b_1^n, \cdots, b_K^n)$, K being the number of one-dimensional grid points, by a discrete summation over the time and space domains :

$$< a^n, b^n >= \sum_{k=1}^{K} a_k^n b_k^n \qquad (12)$$

To simplify our presentation, we present the inverse problem with measurements data with only one thermocouple sensor, point m in the grid. Therefore, the first step in establishing a procedure for the solution of either inverse is thus the definition of an objective (cost) function: it is in our case a least squares performance index *J(p)* that measures the difference between model predictions T_m^n of temperature, given a heat flux parameter *p* value, and measurements temperatures θ_m^n, at point m on the grid, time (n). The quadratic error or cost function j(p), depending on the source parameters p, is defined by :

$$J(p) = J\underbrace{\left(w^1(p), ..., w^N(p)\right)}_{\text{variables } W} = \sum_{n=1}^{N} \left(T_m^n - \theta_m^n\right)^2 \Delta t \qquad (13)$$

with θ_m^n the discrete measured temperature, at time n, point m, and T_m^n the discrete computed temperature vector, at time n, point m.

To minimize this quantity, by optimization algorithm, we need the derivatives of this least squares objective function J(p), with respect to the parameters p.

Adjoint and gradients computations

We introduce the adjoint state matrix $\varphi = (\varphi^{1/2} \cdots; \varphi^{N+1/2})$ adjoint of the direct state matrix w, $\varphi^{n+1/2}$ being a vector (K+1)*1, for all n=0,N. A Lagrangian formalism is used in the minimization of the functional *J(p)* because the estimated dependent variable $w(p)$ appearing in such functional *J(p)* needs to satisfy a constraint, which is the solution of the discrete direct problem. In order to derive the adjoint problem, the governing equation of the direct problem, is therefore multiplied by the Lagrange multiplier, integrated in the space and time domains of interest and added to the original cost functional *J(p)*. The following Lagrangian *L* on these discrete quantities is:

$$L(p,w,\varphi)=L\left(\underbrace{p^1,...,p^N}_{parameter\ p},\underbrace{w^1,...,w^N}_{variables\ w},\underbrace{\varphi^{1/2},...,\varphi^{N+1/2}}_{adjoint\ variables\ \varphi}\right)$$
$$=\sum_{n=1}^{N}\left(T_m^n-\theta^n\right)^2\Delta t$$
$$+\sum_{n=0}^{N-1}\left\langle\varphi^{n+1/2},\frac{w^{n+1}-w^n}{\Delta t}-f\left(w^n\right)-\left(df\right)\left(w^n\right)\left(w^{n+1}-w^n\right)\right\rangle \quad (14)$$

Differentiating the Lagrangian L with first order sensitivity variations, computing δL as function of $\delta p,\delta w,\delta\varphi$, the variations of δL with respect to δw are cancelled with an adequate choice of the adjoint state φ. It leads to the discrete adjoint system[31] in $\varphi^{n-1/2}$ unknown, n going backward from N to 0,

$$\frac{\varphi^{n-1/2}-\varphi^{n+1/2}}{\Delta t}=df^{t}\left(w^{n-1}\right)\varphi^{n-1/2}$$
$$+\left[\left(d^2f\right)\left(w^n\right)\left(w^{n+1}-w^n\right)\right]\varphi^{n+1/2}+2\left(T_m^n-\theta_m^n\right)^2\Delta t \quad (15)$$
$$w^{N+1/2}=0 \qquad N\geq n\geq 0$$

With this particular choice of φ, the gradient of the cost function is simply obtained by :

$$\nabla J=\frac{\partial J}{\partial p}=\frac{\partial L}{\partial p} \qquad (16)$$

Note that that $\left(d^2f\right)\left(w^n\right)$ is a tensor of dimension (K+1)*(K+1)*(K+1), and $\left[\left(d^2f\right)\left(w^n\right)\left(w^{n+1}-w^n\right)\right]$ is a square matrix (K+1)*(K+1). We note also that the adjoint problem involves final conditions given instead of the initial conditions (direct problem): it has to be numerically solved by integrating backward in time as a terminal value problem. The final condition, not detailed here, simply results from the differentiation of (14).

The variations of δL function of δp leads to the expression of the discrete gradients:

$$\frac{\partial J}{\partial p}=\sum_{n=0}^{N-1}\left\langle\varphi^{n+1/2},-\frac{\partial f}{\partial p}\left(w^n\right)-\frac{\partial df}{\partial p}\left(w^n\right)\left(w^{n+1}-w^n\right)\right\rangle \quad (17)$$

Note that $\frac{\partial f}{\partial p}\left(w^n\right)$ is a tensor (K+1)*N, $\frac{\partial df}{\partial p}\left(w^n\right)$ is a tensor (K+1)*(K+1)*N, $\frac{\partial J}{\partial p}$ is a vector 1*N. It can be shown[28] that gradients appeared as combination of direct and adjoint discrete quantities. We won't get into more detailed expressions, because the exact developed terms are quite complex and too big to be described here, the point being the method main principles and the corresponding applications.

Optimization Minimization algorithm

Once the gradient of cost function is computed, we can now apply an iterative inverse procedure minimizing *J(p)* to obtain an estimation of the unknown parameter optimal function p_{opt}. We will use the combination of a gradient steepest descent method at the beginning of minimization and a Quasi Newton method to finish the minimization.

The basic idea of the gradient Steepest Descent Method[32] is to move downwards on the objective function *J(p)* along the direction of highest variation, in order to locate its minimum value. Therefore, the direction of descent is given by the gradient direction, since it is the one that gives the fastest increase of the objective function. Usually the steepest-descent method starts with large variations in the objective function and good initial exploration steps, but, as the minimum value is reached, the convergence rate becomes very low. The algorithm is (18) :

- $p=q_0$ is the initial guess parameter, and *r*, the number of the optimizer iteration has the value r=1, Nop being the maximum number of optimizer iteration.
- $d_r=\frac{\partial J}{\partial q_r}$ gives the descent direction
- $p=q_{r+1}=q_r+\mu_r d_r$ leads to p parameter updating with the descent coefficient μ_r chosen to satisfy the steepest descent of the J(q) cost function $\mu_r=Inf_\mu\ J\left(q_r-\mu d_r\right)$.

When steepest gradient method does not converge any more, the idea is to pursue the optimization process with a second order Quasi Newton method[33,34], which has a strong local convergence. In these types of methods, the Hessian second derivative matrix is approximated in such a way that it does not involve the computation of costly second derivatives. Usually, the approximations for the Hessian are based on first derivatives (gradients) and it accelerates the convergence locally.

Starting with an initial guess for the estimated parameter $p=q_0$, and with an initial matrix H_0^{-1} which is an approximation for the inverse of the Hessian, a Quasi-Newton Broyden Fletcher Goldfarb Shanno (BFGS) optimizer is used to update the parameter value $p=q_r$ at the optimizer step *r*, and the value of H_0^{-1}, until the number of total steps *Nop* of the optimizer is

reached. We stops the process before if an optimal p_{opt} parameter is found, which causes the gradients to vanish (at least a local minimum of J(p)). The BFGS algorithm is the following (19):

- $p = q_0, H_r = H_0$, are the initial guess parameter and Hessian, r is again the current step of optimizer and N_{op} the total number of optimizer iterations.
- $d_r = -H_r^{-1}\dfrac{\partial J}{\partial q_r}$ gives the descent direction
- $H_r = H_{r-1} + z\left(q_{r-1}, q_{r-2}, \dfrac{\partial J}{\partial q_r}, \dfrac{\partial J}{\partial q_{r-1}}, H_{r-1}\right)$ updates the Hessian approximated matrix, with z a function not explicited here
- $p = q_{r+1} = q_r - \mu_r d_r$ allows the parameter updating with the descent coefficient μ_r chosen to satisfy the steepest descent of the *J(q)* cost function $\mu_r = Inf_\mu\ J(q_r - \mu d_r)$.

IV. Inverse problem computation using automatic differentiation

To compute numerically the adjoint and gradient discrete quantities for the inverse problem in heat convection coefficient, we have also used the Automatic Differentiation (AD) engine tool, Tapenade, developed at INRIA Sophia-Antipolis by the Tropics team[24]. Automatic differentiation is a family of techniques for computing the derivatives of a function defined by a computer program (interpreted as computing a mathematical function, including arbitrarily complex simulation codes), for sensitivity and gradient analysis applications[35-37]. The new program obtained is called the differentiated program. Automatic differentiation with adjoint models and gradients computations are used in many fields of science such as pioneering work in meteorology[38-40].

The derivatives of the instructions of a program (elemental operations) are combined according to the chain rule of differential calculus, leading to the two major modes of computing derivatives with AD, the so-called forward (tangent-linear) mode and reverse (cotangent-linear or adjoint) mode.

- The forward mode uses directional derivatives on a given direction vector in the input space (tangent approach. It is appropriate to derive functions with small numbers of independent variables (input).
- The reverse mode uses derivatives starting with the dependent variables (output) and proceeding toward the independent variables (input), and it is computed in the reverse of the original program's order. It is appropriate for functions with small numbers of dependent variables (output) and lots of input independent variables. The reverse mode of automatic differentiation is functionally equivalent to hand written discrete adjoint codes.

The implementation of robust and effective automatic differentiation tools requires advances in compiler technology, graph algorithms, and automatic differentiation theory, and compared with other methods to compute adjoint and gradients, automatic differentiation offers a number of advantages:

- Accuracy: unlike finite difference approximations, derivatives computed via automatic differentiation exhibit no truncation error.
- Reduced software costs: automatic differentiation eliminates the time spent developing and debugging derivative code by hand, or experimenting with step sizes for finite difference approximations.

We have applied these techniques to our inverse thermal problem, considering that the flow of instructions in the direct program (Monopyro direct code), can be schematically represented as sequential instructions $(Inst)^{n+1}$ to compute the direct state variables w^{n+1} given the parameter p

$$w^{n+1} = (Inst)^{n+1}\left[w^n, w^{n-1}, \cdots\cdots, p, \cdots,\right],\ n = 0,..,N \quad (20)$$

$(Inst)^{n+1}$ are discrete functions (that could be non linear functions, recursive functions or interpolated tabulated functions) of discrete temperature and ablation variables. The final output of the program is the discrete cost function $J(p) = J(w(p)) = J\left(\left(w^1,...,w^N\right)(p)\right)$. The adjoint code in φ variables is built by automatic backward differentiation of the output J versus w direct state variables, following and analyzing the flow of instructions in the direct program, and the dependences in w. The gradient computation of $J(p)$ versus p parameter is built by automatic backward differentiation of the output $J(p)$ versus p parameter, also following the flow of instructions in the direct program and analyzing the flow dependences in p. It can be shown again that the gradient result depends on the w direct state variable and the φ adjoint state variable.

V. Numerical results

We now present some applications of inverse problem of the estimation of time domain surface heat convection coefficient for thermally degradable material, on a one-

dimensional slab of thickness e, by using time domain temperature measurements taken below the boundary surface, at a given thermocouple position, during a time interval. As mentionned before, the inverse problem is formulated as a minimization problem involving an objective functional, through an optimization loop. We start the minimization loop by an initial guess on convection coefficient and try to restitute the measurements. In all the following curve results legends, INI stands for initial guess of the convection coefficient, NUM for reconstruction obtained at the end of optimization process, and OBS for the reference solution of the convection coefficient (when this targetted result is known) or for the corresponding measurements, input of inverse method. The final time is denoted by t_f.

We first define two test configurations on measurements:

- Synthetic measurements: the estimated temperatures are obtained from the solution of the direct problem, by using a given well known convection coefficient $\alpha_0(t)$. We want to restitute by inversion this coefficient.

- Noise measurements : the measurements may contain random errors, which are assumed here to be
  - additive, uncorrelated, normally distributed, with zero mean and known standard deviation (2%)
  - additive, uncorrelated, uniformally distributed, with zero mean and known standard deviation (5%)

Here, we want to see the effect of adding this noise to synthetic measurements on the reconstruction of convection coefficient $\alpha_0(t)$, in order to test the stability and robustness of the inverse method.

Moreover, we define now two similar quality estimators for inverse problem :

- A good estimator for the quality of restitution of temperature measurements is the RMS_T error: Root Mean Square error between the θ_m^n measured temperature and the reconstructed temperature $Topt_m^n$, at sensor m, for the optimal inverse solution p_{opt} :

$$RMS_T = EQM = \sqrt{\frac{\sum_{n=1}^{N}\left(Topt_m^n - \theta_m^n\right)^2}{N}} \qquad (21)$$

- A good estimator for the quality of restitution/identification of convection coefficient is the RMS_p error between the reference α_0 convection coefficient and the reconstructed optimal p_{opt} :

$$RMS_p = \sqrt{\frac{\sum_{n=1}^{N}\left(p_{opt}^n - {\alpha_0}^n\right)^2}{N}} \qquad (22)$$

Theses tests have been realised to address the problem of fluxes identification on a carbon/resin material. To ensure the method, we first tried to examine the effects of pyrolysis (test 1) and ablation (test 2) separately, then we worked on the real ablating and pyrolysing material (test 3), then we applied the new method to operationnal cases, such as the quite well known ARD (Atmospheric Reentry Demonstrator, test 4 with a different material: alestrasil), or the more relevant arc plasma torch test on the considered carbon/resin material, where the fluxes are very high and the flow conditions better known and where some fluxmeters measurements are also available (test 5).

Test 1 : Identification of virgin material : without ablation , x0=1.3 mm

We use synthetic data (errorless measurements). We start (INI) with a bad initial guess half value of convection coefficient, with sharp discontinuity. Fig. 1 shows a good agreement for the reconstruction (NUM) of the convection coefficient, compared to the reference convection coefficient (OBS), with the inverse code developed in section III ("hand computed" gradients and adjoints), except near the final time. The RMS error on the flux is 0.04.

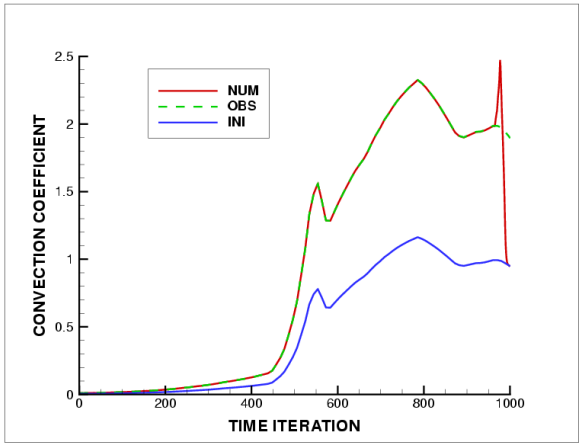

Figure 1. Test 1 : Flux Identification of virgin material : without ablation , x0=1.3 mm

The results shown in Fig. 2 were obtained with the inverse code developed in section IV (Automatic Differentiation tool was used) and are very correct too.

Near final time, the value of the estimated flux has very little influence on the temperature in the material, at x0. Even if the flux is worse evaluated at the end, the impact on the corresponding solution is not visible.

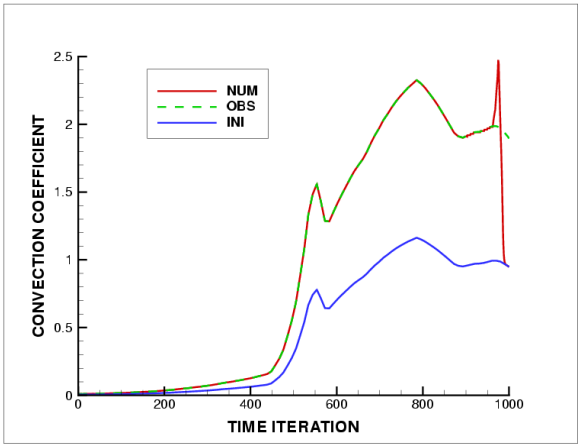

Figure 2. Test 1 : Flux Identification of virgin material : without ablation, x0=1.3 mm Automatic Differentiation tool

Fig. 3 shows that the RMS error on temperature obtained at the end of optimization process (also using the Automatic Differentiation tool), is very low (0.01), and we can observe the change in optimizer (iteration 25), switching from gradient steepest descent at the beginning, to Quasi Newton after. The gain in convergence is promising, after 60 optimizer iterations.

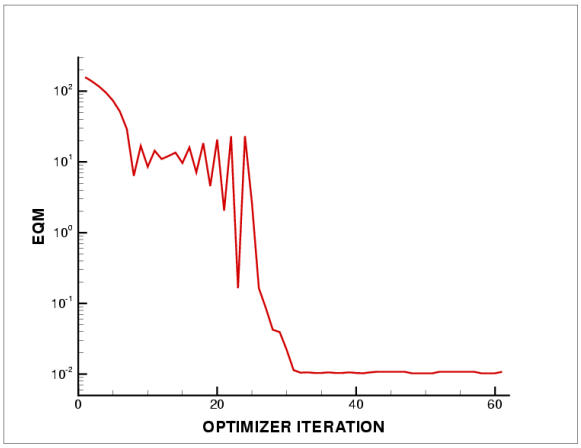

Figure 3. Test 1 : Temperature RMS error Virgin material : without ablation , x0=1.3 mm Automatic Differentiation tool

Test 2 : Identification of High Flux with ablation, Carbon/Resin material , x0=2.6 mm

It is a quite difficult test case, with high fluxes. In Fig. 4, a good agreement in the reconstructed convection coefficient value is obtained, except at final time, with initial half guess and using synthetic data (errorless measurements). The RMS error on the flux is 0.06.

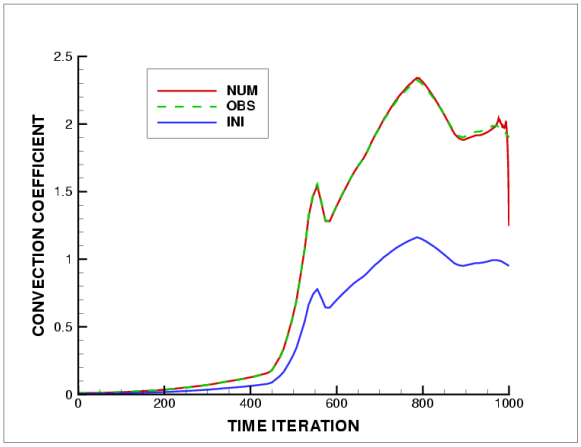

Figure 4. Test 2 : Identification of High Flux with ablation, x0=2.6 mm

Fig. 5 shows that the RMS error on measured temperature obtained at the end of optimization process is very low (0.7), after 70 optimizer iterations.

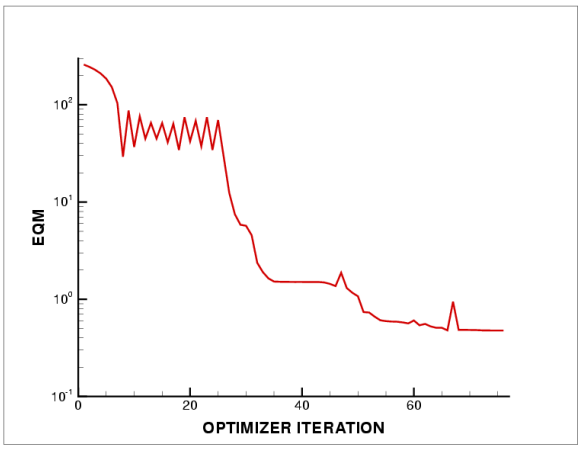

Figure 5. Test 2 : RMS error on temperature : with ablation , x0=2.6 mm

Fig. 6 shows results in the convection coefficient obtained, with initial half of the value, additive, uncorrelated, normally distributed, zero mean and known standard deviation (2%) noise. The RMS error on the flux is 0.105, which is satisfactory.

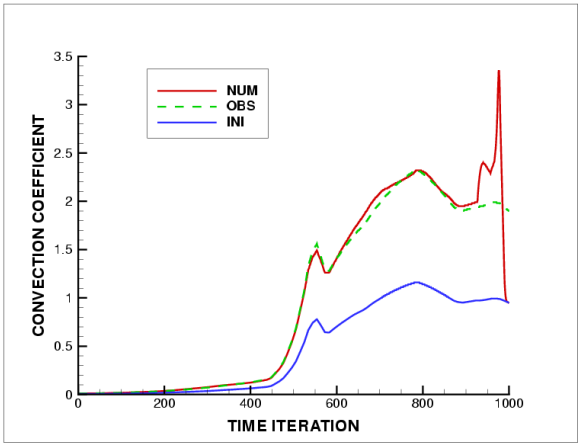

Figure 6. Test 2 : Identification of High Flux with: with ablation 2% normal noise , x0=2.6 mm

Fig. 7 shows results in the convection coefficient obtained, with initial half of the value, additive, uncorrelated, uniformally distributed, zero mean and known standard deviation (5%) noise. The RMS error on the flux is 0.125.

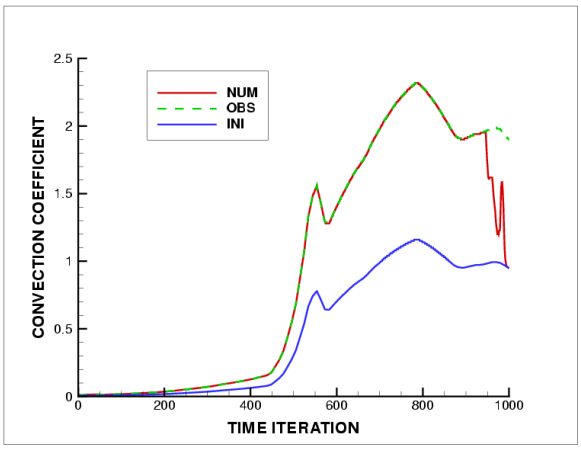

Figure 7. Test 2 : Identification of High Flux with ablation, 5% uniform noise, x0=2.6 mm

Test 3 : Identification of High Flux with ablation and pyrolysis, Carbon/Resin material x0=4.2 mm

We now examine the present inverse analysis approach for a difficult test case, with high fluxes, ablation, pyrolysis, and deep thermocouples location and synthetic measurements on a "real" material.

Successful results are obtained in the reconstructed convection coefficient and displayed on Fig. 8, with a RMS error on the flux of 0.07.

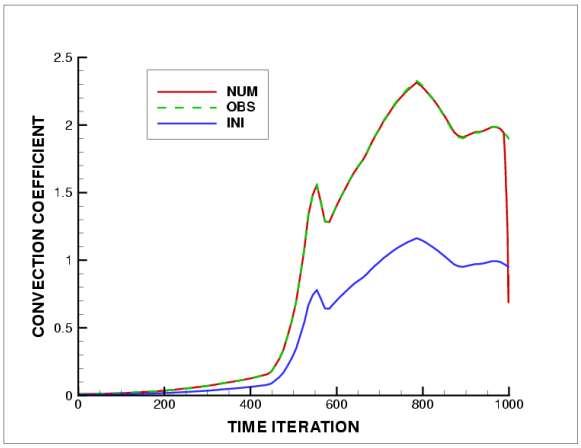

Figure 8. Test 3 : Identification of High Flux with ablation and pyrolysis, x0=4.2 mm

Fig. 9 shows that the RMS error on temperature at the sensors obtained at the end of optimization process is very low (0.9), after 75 optimizer iterations.

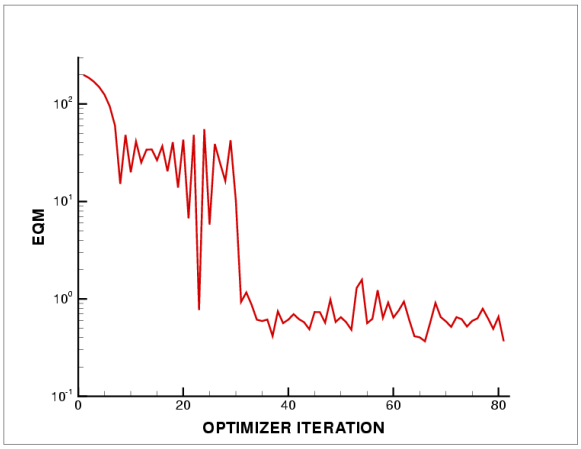

Figure 9. Test 3 : Temperature RMS error
High Flux with ablation and pyrolysis, x0=4.2 mm

Test 4 : ARD Test case

We now examine the present inverse analysis approach for the ARD flight test case. The Atmospheric Reentry Demonstrator (ARD) was a suborbital reentry test flown on the third Ariane 5 flight. ARD was launched in october 1998 from Kourou, French Guyana, by an Ariane 5 and splashed down 1 hour 41 min. after liftoff. It was recovered and transported in EADS Astrium Aquitaine plant for expertise. More than 200 different parameters were recorded during flight. After ARD recovery, a preliminary analysis of recorded data has been performed.

A picture of the recuperation of the capsule is given on Fig. 10. The heat shield (Fig. 11) has been expertise (Fig. 12) after the flight.

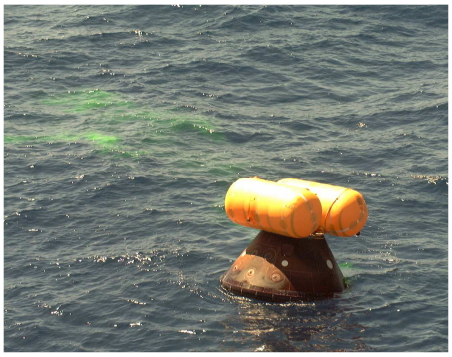

Figure 10. ARD sea landing

Figure 11. ARD heat shield

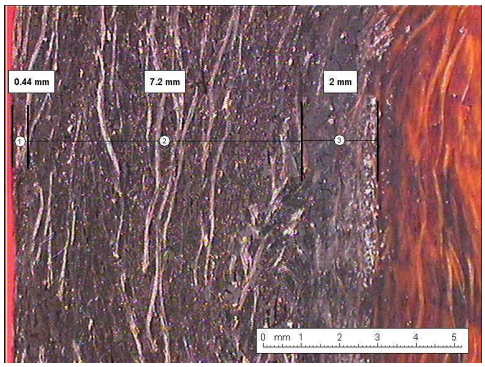

Figure 12. ARD thermocoil

Successful results are obtained in the reconstructed flux (Fig. 13), which are very similar to those obtained before (see Fig. 14 and [23]).

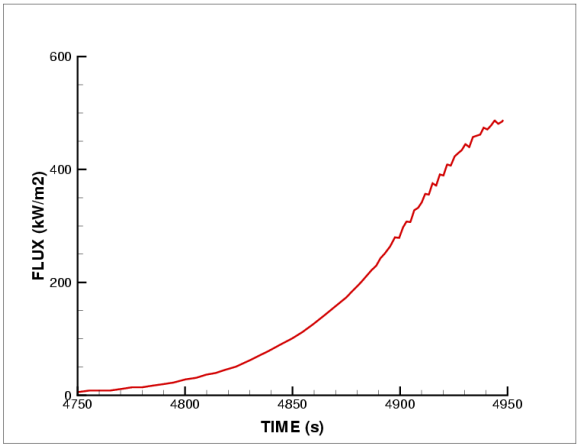

Figure 13. ARD heat flux restitution

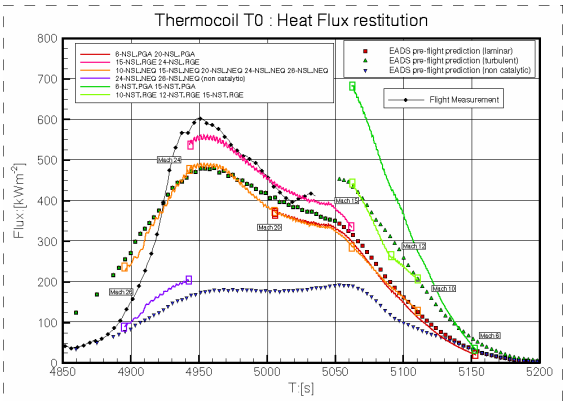

Figure 14. ARD post flight analysis : heat fluxes, courtesy of [23]

Test 5 : Operational test case (Plasma Jet case)

This case has been investigated to improve the robustness on an industrial problem where many experimental data were available. The industrial applications are straight forward. The plasma jet facility of the Astrium's Aquitaine plant is shown on Fig. 15, with the schematic principal of a plasma torch. The experimental test facility uses four coupled plasma torchs.

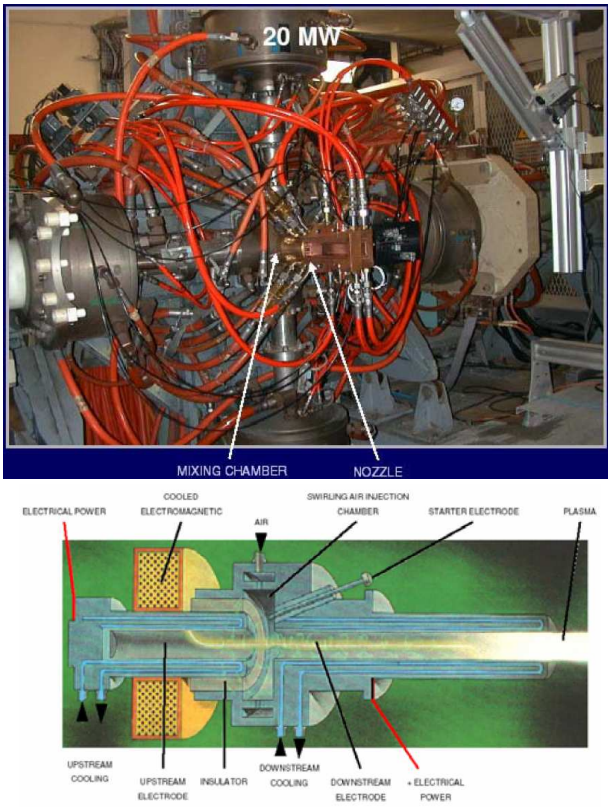

Figure 15. Plasma jet facility

We show Fig. 16 the sensibility to the inverse convection coefficient problem, for two different initial guess on the flux. The temperature restitutions, as shown Fig. 17, are very similar at the sensors, for these two different solutions.

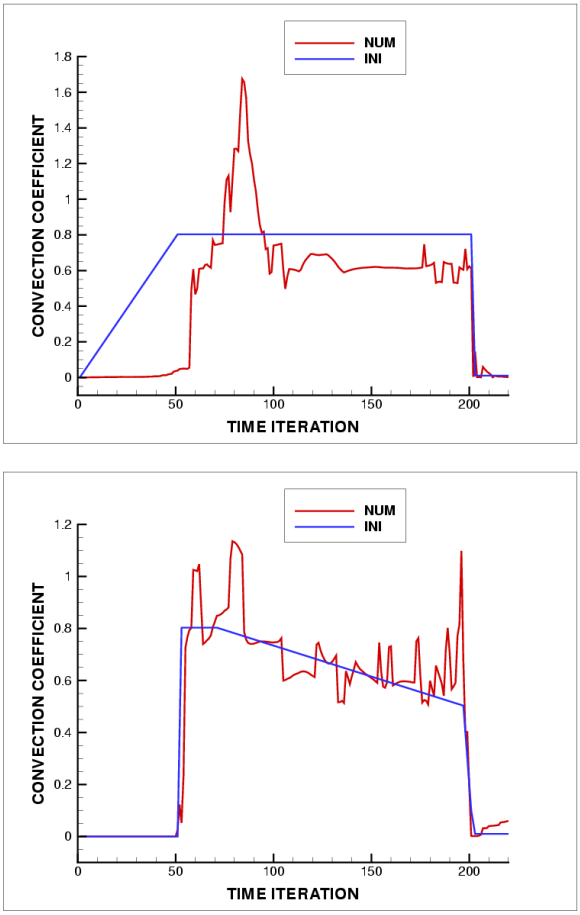

Figure 16. Test 5 Flux identification Plasma Jet test case - Two different initial guess

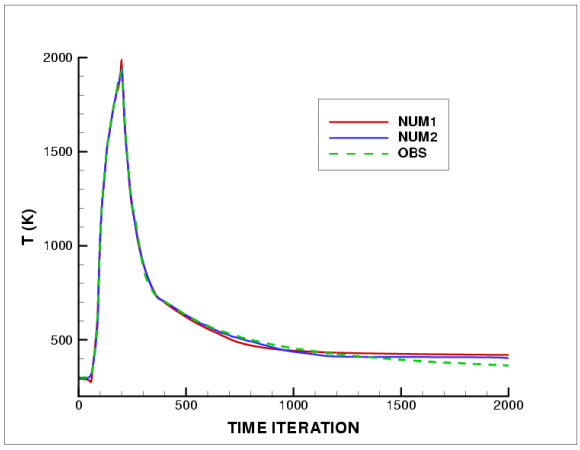

Figure 17. Test 5 Temperature Restitution Plasma Jet test case - Two different initial guess

VI. Conclusion

Motivated by atmospheric re-entry of aerospace vehicles and Thermal Protection System dimensioning problems, this article is concerned with inverse analyses of highly dynamical heat fluxes. It addresses the inverse problem of using temperature measurements to estimate the heat flux convection coefficient, at the surface of ablating materials.

The inverse problem is formulated as a minimization problem involving a least square problem functional, through an optimization loop. An optimal control formulation (Lagrangian, adjoint and gradient computations) is then applied and developed, using an inverse software Monopyro which was developed at EADS Astrium-ST Les Mureaux, and which is a transient one-dimensional thermal code, with ablative surface and Gear integration scheme.

Several validation test cases, using synthetic, noisy on-ground and in-flight data temperatures measurements are carried out, by applying the results of the minimization algorithm. Main results are:

- Validity of the inverse formulation for the description of the temperature and ablation variables evolution
- Improvement by using a combined gradient steepest descent method at the beginning of minimization process and Quasi Newton method to finish the minimization,
- Convection coefficient restitution has been improved for hard cases (with great ablation) for fluxes functions containing sharp corners and discontinuities,
- Successful test case on carbon/resin material with high heat fluxes and large magnitudes, ablation including pyrolysis effects, and opartional data,
- Encouraging results with an automatic differentiation tool are also obtained, without ablation

Future works have to be done on the:

- Robustness to initial guess, sensitivity to measurements, number and position of sensors, and application of regularization methods to stabilize noise errors on measurements,
- Implementation of the automatic differentiation tool to generate the inverse code,
- Thermal model uncertainties influences on the accuracy of extracted flight heat flux, athermanous enthalpy identification,
- Validations on aerothermal flight measurements.

Acknowledgments

This work was sponsored by EADS Astrium-ST. The authors would like to acknowledge Benoit Fourure, Antonio Rivas, Jacques Soler, Philippe Tran, (EADS-Astrium-ST) and Eric Duceau, Isabelle Terrasse, (EADS-IW) for their efficient support.

References

[1] Macret, J.L., Leveugle, T., "The Atmospheric Reentry Demonstrator program : overview and flight results", IAF-99-V.2.10, *50th International Astronautical Congress*, 4-8 Oct 1999/Amsterdam, The Netherlands.

[2] Macret, J.L., Paulat, J.C., Tran, P., Rolland, J.Y., and Steinkopf, M. "Post Analysis of the atmospheric reentry demonstrator flight" *51th International Astronautical Congress IAF-00-V.2.05s*, Rio de Janeiro, Brazil, October 2000.

[3] Boukhobza, P., Paulat, J.C., Riccardi, S., Soler, J.,Tran, P., Véronneau, Y., and Walpot, L.,"Recent re-entry flight experiments lessons learned – ARD", *Flight Experiments for Hypersonic vehicle development, Von Karman Institute for Fluid Dynamics*, 24 - 27 October 2005.

[4] Epherre, J.F. and Laborde, L. "Pyrolysis of carbon phenolic composites", *Fourth International Symposium Atmospheric Reentry Vehicles and Systems* – Arcachon – 21 au 23 mars 2005.

[5] Velghe, A. Duffa, Nguyen-Bui, N-T-H., and Dubroca, B., "Modeling of the Surface State of Ablatable Material by Reaction-Diffusion Phenomenon", *AIAA/CIRA 13th International Space Planes and Hypersonics Systems and Technologies Conference*, 16 - 20 May 2005 Centro Italiano Ricerche Aerospaziali (CIRA), Capua, Italy, 2005.

[6] Bouilly, J-M., Dariol, L. and Leleu, F. "Ablative Thermal Protections for Atmospheric Entry. An Overview of Past Missions and Needs for Future Programmes", *5 thEuropean Workshop Thermal Protection Systems and Hot Structures*, 17/19 May 2006 Noordwijk, The Netherlands.

[7] Boursereau, F., Donnart, P., Bouffet, S., Astier, JC, Jullien P., and Foltyn, M. "Theoretical and experimental investigations on a new configuration arc plasma torch", 6*st International Symposium - Atmospheric Reentry Vehicles and Systems* ; Arcachon, France, 21 au 23 mars 2005.

[8] Dubroca, B., Duffa, G., and Leroy, B. "Heterogeneous Reactions on TPS Surfaces: General Derivation and Equilibrium Limit", *AIAA/CIRA 13th International Space Planes and Hypersonics Systems and Technologies Conference*, 16 - 20 May 2005 Centro Italiano Ricerche Aerospaziali (CIRA), Capua, Italy, 2005.

[9] Cosson, A.E., Thivet, F., Soler, J., Tran, P., Spel, M., Dieudonné, W., Paulat, J.C., Parmpolini, M., and Moulin, J., "Pre-X Aerothermodynamics Implications at System Level", *Fourth International Symposium Atmospheric Reentry Vehicles and Systems* – Arcachon – 21- 23 mars 2005.

[10] Wright, M., Milos, F., and Tran, P."Survey of Afterbody Aeroheating Flight Data for Planetary Probe Thermal Protection System Design ", *38th AIAA Thermophysics Conference*, June of 2005 in Toronto, Ontario Canada.

[11] Bouilly, J-M., "Thermal Protection System of the Huygens Probe during Titan Entry: Flight Preparation and

Lessons Learned", *5 thEuropean Workshop Thermal Protection Systems and Hot Structures*, 17/19 May 2006 Noordwijk, The Netherlands.

[12] Collinet, J., Brenner, P., and Palerm, S., "Dynamic stability of the HUYGENS probe at Mach 2.5" , *Aerospace Science and Technology* Volume 11, Issues 2-3, March-April 2007, Pages 202-210.

[13] Beck J.V., B Blackwell, B., Inverse Heat Conduction: Ill-Posed Problems, *CR St Clair - A Wiley* {Interscience Publication, New York, 1985.

[14] Machado, H.A. and Orlande H.R.B. "Inverse analysis for estimating the timewise and spacewise variation of the wall heat flux in a parallel plate channel", International Journal of Numerical Methods for Heat & Fluid Flow, 1997.

[15] Walker, D.G. and Scott, E.P. ``A Method for Improving Two-Dimensional High Heat Flux Estimates from Surface Temperature Measurements," *proceedings of the 32nd AIAA Thermophysics Conference*, AIAA-97-2574, Atlanta, GA, June 1997.

[16] Li H. Y. and Yan, W. M., "Estimation of Wall Heat Flux in an Inverse Convection Problem," *AIAA Journal of Thermophysics and Heat Transfre*, Vol. 13, No. 3, pp. 394-396, 1999.

[17] Blanc, G., Beck J.V., and Raynaud, M., " Solution of the inverse heat conduction problem with a time variable number of future temperatures ", *Numerical Heat Transfe*r, Part B, Vol. 32, pp.437-451,1997.

[18] Hoornaert, A., Pelissier, C., Le Sant, Y., Thivet, F., Millan, P., "On-ground validation of rear-face thermography to measure surface heat fluxes in hypersonic flows", *6th International Symposium on Launchers Technologies* – Munich (Germany) – 8 au 11 nov. 2005.

[19] Lions, J.L., *Contrôle Optimal des Systèmes gouvernés par des équations aux Dérivées Partielles*, Dunod Paris, 1968.

[20] Alestra, S., Terrasse, I. and Troclet, B., "Inverse Method for Identification of Acoustic Sources at Launch Vehicle Lift-off", AIAA *Journal, Vol 41*, Number 10, pages 1980- 1987, October 2003.

[21] Troclet, B, Alestra S., Terrasse, I. Jeanjean, S., and Srithammavanh, V., "Identification of Overpressure Sources at Launch Vehicle Liftoff Using an Inverse Method", AIAA Journal of Spacecraft and Rockets 2007 0022-4650 vol.44 no.3 (597-606).

[22] Rivas, A., "Monopyro, dépouillement des thermobobines : Monopyro software équations*", Aerospatiale Technical Internal note*, 2000.

[23] Tran, P., and Soler, J. "Atmospheric reentry demonstrator, Post-Flight Analysis : Aerothermal Environment", *2nd International Symposium - Atmospheric Reentry Vehicles and Systems* ; Arcachon - March 2001.

[24] Hascoët L., Greborio, R.M. , and Pascual V., "Computing Adjoints by Automatic Differentiation with Tapenade ", *Ecole CEA-EDF-INRIA "Problèmes non-linéaires appliqués*", Paris, 2002.

[25] Dubois, F., and Rivas, A. "Volumes finis à l'Aérospatiale", *Ecole CEA EDF-INRIA "Méthodes de Volumes Finis*", 28 - 30 October 1992.

[26] Bouffet, S. "Document Plan Logiciel : Software Guide Documentation Code BE13" LY211 n° 138 717, *EADS LV Technical Internal note*, 2002.

[27] Roache, P. J., *Computational fluid dynamics*, Hermosa publishers, 1972, PO Box 8172, Albuquerque.

[28] Collinet, J "Monopyro Technical report on High fluxes results with a new inverse formulation for ablative material" EADS Astrium-ST Technical Internal note, 2007.

[29] Dubois, F., "A Sparse matrix solver for Monopyro inverse code", *EADS Technical Internal note, May*, 2007.

[30] Bamberger, A., Chavent, G. and Lailly, P., "About the Stability of the inverse problem in 1D wave equation", *Journal of Applied Mathematics and Optimisation, 5*:1-47, 1979.

[31] Tekitek, M.M., Bouzidi, M., Dubois, F., and Lallemand, P., "Adjoint lattice Boltzmann equation for parameter identification", *Computers & Fluids*, 35 (8-9), 805-813, 2006.

[32] Minoux, M., *Mathematical Programming: Theory and Algorithms*, Chichester: John Wiley and Sons, 1986.

[33] Gilbert, J.Ch., and C.Lemaréchal, C., "Some numerical experiments with variable-storage quasi-Newton algorithms". *Mathematical Programming*, 45 (1989), pp. 407-435.

[34] Bonnans, J.F., Gilbert, J.Ch., Lemaréchal, C., Sagastizabal, C., *Numerical Optimization Theoretical and Practical Aspects*, Springer Verlag, Berlin. (2002).

[35] Griewank, A., "Achieving Logarithmic Growth of Temporal and Spatial Complexity in Reverse Automatic Differentiation", *Optimization Methods and Software*, 1(1):35-54, 1992.

[36] Faure, C., "Quelques aspects de la simplification en calcul formel", Thèse de l'Université de Nice-Sophia Antipolis, 1992.

[37] Faure, C., and Papegay, Y.,"Odyssée User's Guide Version 1.7", Rapport technique, INRIA, 1998, no 224 URL: http://www.inria.fr/rrrt/rt-0224.html.

[38] Le Dimet, F., and Talagrand, O., "Variational algorithms for analysis and assimilation of meteorological observations : theoretical aspects", in: *Tellus, 1986*, vol. 38A, p. 97-110.

[39] Talagrand, O.and Courtier, P., "Variational assimilation of meteorological observations with the adjoint vorticity equation. I: Theory", *Q. J. R. Meteorol. Soc.* 1987, vol. 113, no 478, pp. 1311-1328.

[40] Talagrand, O., "The use of adjoint equations in numerical modelling of the atmospheric circulation", *Automatic Differentiation of Algorithms : Theory, Implementation and Application*, A. Griewank, G. Corliss (editors), SIAM, 1991, p. 169-180.